Indian Journal of Chemistry
Vol. 60B, February 2021, pp. 303-320

In vitro anticancer activity of thiazole based β-amino carbonyl derivatives against HCT116 and H1299 colon cancer cell lines; study of pharmacokinetics, physicochemical, medicinal properties and molecular docking analysis

Ajay Manohar Ghatole*[a,b], Mahesh Krishanarao Gaidhane[c], Kushal Radhesham Lanjewar[d] & Kishor Manohar Hatzade[b]

[a] Department of Chemistry, Gov. Institute of Science, Civil line, Nagpur 441 001, India

[b] Department of Chemistry, Dhote Bandhu Science College, Gondia 441 614, India

[c] Department of Chemistry, Shri Lemdeo Patil Mahavidyalaya, Mandal, Kuhi, India

[d] Department of Chemistry, Mohsin Bhai Zawer College, Wadsa, Desaigang, India

E-mail: ajay.ghatole5@gmail.com; kishorhatzade@gmail.com

Received 1 December 2019; accepted (revised) 19 January 2021

The present study describes the synthesis and anticancer evaluation of certain substituted rac-(2S)-2-[(R)-[(4-substitutedphenyl){[4-(4-substitutedphenyl)-1,3-thiazol-2-yl]amino}methyl]cyclohexanone derivatives. The *in vitro* anti-cancer assay indicating substituted β-amino carbonyl derivatives **4g** and **4r** are particularly active in both tests (HCT116 and H1299). The **4f, 4o**, and **4t** are the least functioning; **4m** and **4n** are marginally active; **4b** and **4c** are more cytotoxic when the growth inhibition percent is compared with standard drugs Camptothecin (CPT.), Acyclovir (ACV), Cisplatin (CDDP.), Vinblastine (VBL) and Trichothecene (TCT.). Among them, 2-((4-*p*-tosylthiazol-2-ylamino)(4-hydroxyphenyl)methyl) cyclohexanone **4u** exhibits selective cytotoxicities for IC_{50} μg/mL against HCT116 and H1299, respectively. Simulation of virtually designed 21 compounds has been studied for active binding sites of Crystal Structure of the Cancer Genomic DNA Mutator APOBEC3B (PDB ID- 5CQD) enzyme using molecular modelling of protein-ligand interactions. The in-depth sequencing studies reveal that the involvement of APOBEC3B in cancer mutagenesis. For comparison, the binding behaviour of known standard drugs has also studied. The new SwissADME web utensil that gives free access to a pool of quick yet reliable analytical models is presented for physicochemical properties, pharmacokinetics, drug-likeness, and medicinal chemistry. Among them, in-house capable technique, for example, BOILED-Egg, iLOGP, and Bioavailability Radar, are readily available on the web.

Keywords: Thiazole derivatives, HCT116, H1299, APOBEC3B (PDB ID- 5CQD), SwissADME, BOILED-Egg, bioavailability radar

The principal aim of our effort is the discovery of novel cytotoxic and anticancer agents with fewer side effects of standard drugs (Figure 1). The three main treatments of neoplastic diseases comprise surgery, radiotherapy, and chemotherapy; this last one is the most limited, with a rate value of 5-10% of total healing. There is numeral difficulty with the safety profile and efficacy of chemotherapeutic agents. The attempts to create a new drug, which can be used further in the treatment of any disease is a formidable challenge. Many failures accompany development. It is always necessary to have a lot of creativity, intelligence, and overall good team work for better results[1].

Cytotoxic primarily affects the rapidly dividing cells, so it does not target the cancer cells, which specified in the resting phase. Finally, cytotoxic are associated with a high incidence of adverse effects. The typical examples consist of bone marrow suppression, alopecia, mucositis, nausea, and vomiting. Several publications reported on Mannich ketones as potential cytotoxins[2-5].

Some Mannich bases synthesized from thiazole or its derivatives containing aromatic or heterocyclic rings. It was estimated that at least 35% of β-amino carbonyl derivatives related articles are published in pharmaceutical journals. They are known through use in polymers, resins, the surface at active agents[6], detergent additives[7] antioxidants, and diuretic[8]. They have a broad range of biological activities, including antipsychotic[9], oxytocin[10], anticonvulsant[11], centrally acting muscle relaxant[12], anticancer[13,14], antimalarial[15], antiviral[16], anti-tubercular, anti-bacterial and anti-fungal[17]. Furthermore, β-amino

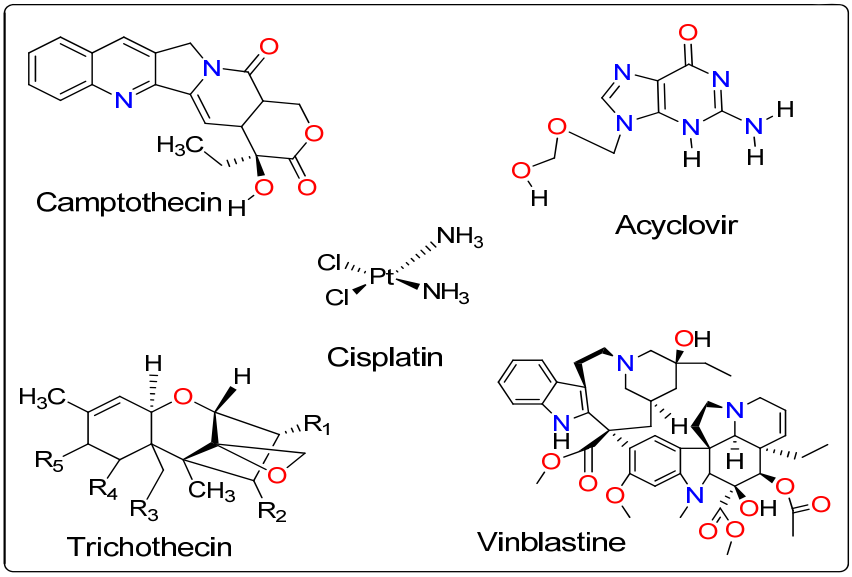

Figure 1 — Molecular structure of the standard drugs

carbonyl derivatives of various bioactive compounds have been prepared as prodrugs utilizing overwhelming some boundaries.

The synthesis of asymmetric Mannich reaction is one of the most critical results in the formation of C-C bonds in the simulated organic chemistry used during the construction of enantiomerically augmented nitrogenous molecules and their derivatives. The development of asymmetric Mannich reaction has been encouraged by a wide variety of natural products and drugs possessing optically active, nitrogen-containing molecules, which have attracted attention from synthetic chemists and the pharmaceutical industry[18-23]. To support the above study, we have to carry out the *in vitro* anticancer activity of the synthesized compounds against HCT116 and H1299 cancer cell lines with the help of Dr D. P. Manivasakam, Director, Biology Indus Pharmaceuticals 25 Olympia Avenue Suite K-600, Woburn, MA, USA.

For the additional support to study, we have carried out the computational docking against the Cancer Genomic DNA Mutator APOBEC3B (PDB ID-5CQD). A few years ago, scientists discovered a distinctive mutagen that poses in our cells: APOBEC, a protein that habitually functions as a preserving agent against viral infection. APOBEC3B is a member of the astronomical family of zinc-dependent DNA deaminases that to adherent the cytosine that works typically as a nuclear-localized restriction factor of DNA-based pathogens bases into uracil in single-stranded DNA and RNA[24,25]. APOBEC is a useful yet fatal, intrinsic cellular protein. Typically meant to fight viruses, it has only the power of modifying single-stranded DNA. Human double-stranded DNA, therefore, should not be altered. But scientists observed that mutations brought by APOBEC found in many tumorous cells, throughout the genome[26]. The APOBEC3B mutagenesis accounts for the most clustered and dispersed cytosine deamination that causes mutation in cancer. The cause of the disease is because of abnormal cell growth, which docks DNA mutations, electrifying during the DNA replication process. If the regular miscue takes place without having any deadly effect on the organism, a specific part of the genome may be affected by which causes the accumulation of the mutant cell, which then enters the body. Today geneticist has conceived how APOBEC takes supremacy of a weakness in our DNA approximation process to check mutations in our genome[27].

Notwithstanding the above computational examination, we additionally utilize advance and new methodology, *i.e.*, Swiss absorption, distribution, metabolism, and excretion study. Swiss ADME is an excellent and exhaustive site kept running by the Swiss foundation of bioinformatics (SIB), which gives bioinformatics administrations and assets to researchers around the world. SIB has more than 65 bioinformatics research gatherings and 800 researchers from the real Swiss schools of advanced education and research institute. Swiss ADME

empowers the appraisal of ADME parameters of medication applicants and small molecules and gives data that permits early hazard evaluation in the drug improvement process. Eminently, swissADME provides a stage to evaluate Lipinski's rule of five[28] for medication resemblance of oral bioavailability. Drug-likeness is an unpredictable equalization of molecular properties and structural features that decide if an unfamiliar molecule resembles the known drug. These molecular properties incorporate hydrophobicity, electronic dispersion, and hydrogen bonding attributes molecular size and adaptability. SwissADME includes the 'BOILED-Egg' assessment[29] that foresee gastrointestinal captivation (HIA) and efflux/maintenance by P-glycoprotein (Pgp). Also, the blood-brain barrier (BBB) infiltration and Cytochrome P450 (CYP) enzyme substrate-restraint expectation can make.

Overall, these *in vitro* and computational studies provide a framework for further mechanistic studies and the development of novel anti-cancer drugs to inhibit this enzyme. Among these methods, docking has been used widely in drug designing for cancer[30,31] dampen tumour evolution, and minimize adverse outcomes such as drug resistance and metastasis. So, it better to limit the present study to some selected cancer macromolecules. The role of these macromolecules well studied by different scientists from time to time[32,33], and their inhibition justifies the role in anticancer potential.

Furthermore, there are increasing concerns about environmental effects, which require synthetic manipulation that minimize the use of hazardous chemicals. Many strategies have devised and investigated, mainly by replacing the traditional organic with other non-toxic solvents. Recently, ionic liquids have attracted broad interest as excellent alternatives to organic solvents, due to there desirable properties, such as non-flammability, no measurable vapour pressure, low toxicity, reusability, low-cost and high thermal stability[34-38]. In addition to the polar properties of ionic liquids, they are non-coordinating, which avoids any undesired solvent binding in pre-transition states, and hence offers excellent advantages for asymmetric synthesis. As a result, ionic liquids considered promising alternative solvents for organic reactions. Over the past few years, these liquids have generated a significant amount of interest[39-49].

Result and Discussion

In this study, we observed that substituted thiazole-based β-amino carbonyl derivatives**4d**, **4g**, **4i**, **4k**, **4l**, **4r**, **4s**, and **4u** are more cytotoxic than the growth inhibition% compared with standard drug's CPT., ACV., CDDP., VBL., and TCT. Indifferent human cancer cell lines with several p53 statuses. Besides, asymmetric synthesis of various functional molecules is one of the essential tasks in modern organic synthesis[50]. Therefore, it is crucial to develop efficient a symmetric C-C bond forming reactions.

The IR spectra of compounds **4a-u** showed a peak at 3098-3150 cm^{-1} due to –NH function. A sharp band observed at 1680-1720 cm^{-1} corresponding to the carbonyl (-C=O) function derived from cyclohexanone structure.

The ^{1}H NMR spectra of compounds **4a-u** displayed an additional signal at 6.53 ppm due to the –NH linkage derived from a thiazole moiety with aldehyde and cyclohexanone, while the sign due to the $–NH_2$ group of thiazole structure did not appear. The singlet for $–OCH_3$ observed at 3.6 ppm integrated for three protons in ^{1}H NMR spectra of compounds **4a-h**. The ^{1}H NMR spectra of compounds **4i-p** and **4q-u** revealed singlets at 9.1 ppm and 1.3 ppm integrating for a single proton of –OH group and three protons of $–CH_3$ group, respectively. Also, $-OCH_3$ group of compound**4b** resonated at 3.84 ppm integrating for three protons as a singlet in the ^{1}H NMR spectrum. Moreover, the signals derived from two $–CH_3$ groups in compound **4c** and **4j** were recorded at 2.3 ppm integrating for three protons. A singlet at 9.1 ppm observed for the Ar –OH group of compound **4u**.

The ^{13}C NMR spectrum of compound **4a** showed aromatic resonances at 126.0, 129.4, and 151.7 for aromatic carbon atoms. Aromatic resonance's signals for -Cl carbon appears at 162.32 for $–OCH_3$, -OH, $-CH_3$ substitution and fused aldehydic aromatic carbon of compound 4a appears at 139.54, 134.14, 130.44, 129.23, 126.51 and 115.48. The carbon of cyclohexanone ring found at 57.22, 39.52, 27.92, 25.65, 23.65, respectively. The peak corresponding to the $–OCH_3$ at 61.9 and the peaks at 62.9 and 64.6 indicated the attachment of cyclohexanone ring *via* aromatic aldehyde with the formation of diastereomer arising from two unresolved chiral centres. The compounds **4a-u** revealed peaks at 211.0-217.3, suggesting the presence of -C=O of cyclohexanone ring.

In this paper, we demonstrate an asymmetric Mannich-type reaction in ionic liquids (Scheme I).

The elemental analysis and molecular ion peaks of compounds **4a-u** were consistent with the assigned structure. The yield and melting point reported in Table I.

Table I — Synthesis of compounds **4a-u**

S. No.	R_1	R_2	R_3	R_4	Time (hr.)	m.p. (°C)	% Yield
4a	OCH_3	Cl	H	H	6	217	85
4b	OCH_3	H	H	OCH_3	6	190	89
4c	OCH_3	H	H	$N(CH_3)_2$	6	185	87
4d	OCH_3	H	H	F	6	188	85
4e	OCH_3	H	H	Cl	6	195	84
4f	OCH_3	H	Cl	H	6	245	84
4g	OCH_3	H	NO_2	H	6	190	84
4h	OCH_3	H	H	H	6	194	83
4i	OH	H	H	OCH_3	6	232	92
4j	OH	H	H	$N(CH_3)_2$	6	212	86
4k	OH	H	H	F	6	232	90
4l	OH	H	H	Cl	6	235	90
4m	OH	H	Cl	H	6	254	91
4n	OH	H	NO_2	H	6	230	89
4o	OH	H	H	OH	6	230	90
4p	OH	H	H	H	6	258	82
4q	CH_3	H	H	OCH_3	6	130	85
4r	CH_3	H	H	Cl	6	124	84
4s	CH_3	H	Cl	H	6	125	83
4t	CH_3	H	NO_2	H	6	125	84
4u	CH_3	H	H	OH	6	126	83

Biological activity of the target molecules

All compounds, as well as the standard drugs (Figure 1), were evaluated *in vitro* against a 2-cell line panel consisting of HCT116 and H1299 colon cancer cell lines, respectively. Results of all the substituted 2-((4-phenyl)(4-(4-phenyl)thiazol-2-ylamino)methyl)-cyclohexanone derivatives **4a-u** are active, out of which most of the methoxy; hydroxy-phenylthiazole (**4a-c**, **e-f**, **h**, **j**, **m)** and methyl-phenylthiazole unit of substituted Mannich derivatives (**4q**, **4t)** exhibited a weak inhibitory activity on the growth of HCT116. The H1299 cell line, all the compounds, shows promising activity. 2-(((4-(4-methoxyphenyl) thiazol-2(3H)-ylidene)amino)(3-nitrophenyl)methyl) cyclohexanone (**4g)** and 2-((4-chlorophenyl)((4-(p-tolyl)thiazol-2(3H)-ylidene)amino)methyl)cyclohexanone (**4r)** were particularly active in both assays; 2-((3-chlorophenyl)((4-(4-methoxyphenyl)thiazol-2(3H)-ylidene)amino)methyl)cyclohexanone (**4f**) and 2-((4-hydroxyphenyl)((4-(4-hydroxyphenyl)thiazol-2(3H)-ylidene)amino)methyl)cyclohexanone (**4o**) were the least functioning; **4m** and **4n** are marginally active. The effect of all new compounds on colon cancer cell lines HCT116 and H1299 was observed, and results depicted in Figures 2-5. Growth inhibition % compared with standard drugs Camptothecin, Acyclovir, Cisplatin, Vinblastine, and Trichothecene. (Table II, Table III and Figures 6-7).

Geometrical conformation

The possible existence of the prepared compounds in various tautomeric forms represented in (Figure 8).

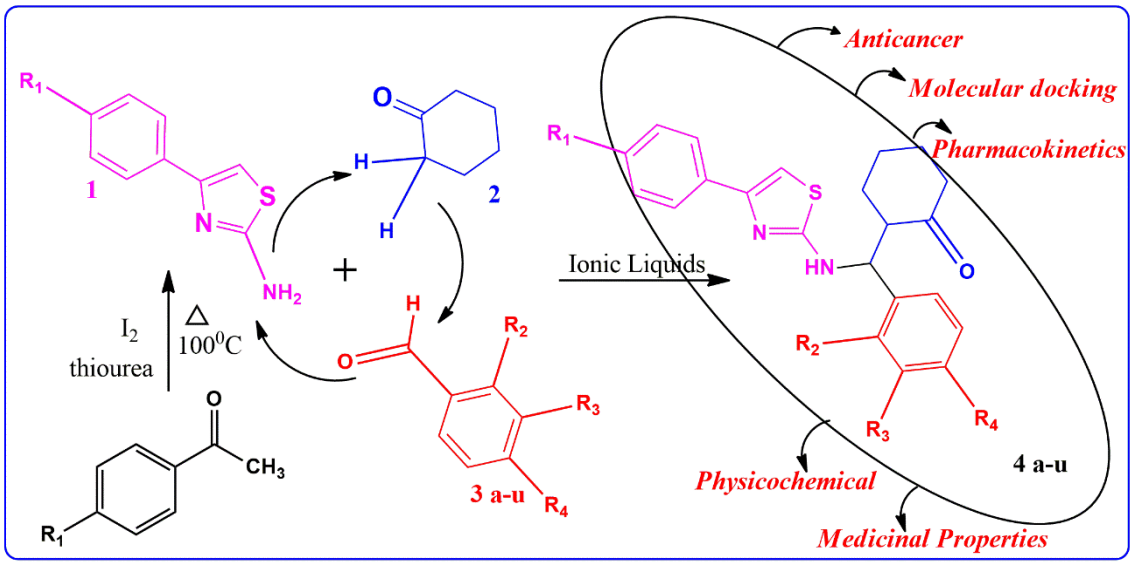

Scheme I — One pot synthesis of thiazole based β-amino carbonyl derivatives

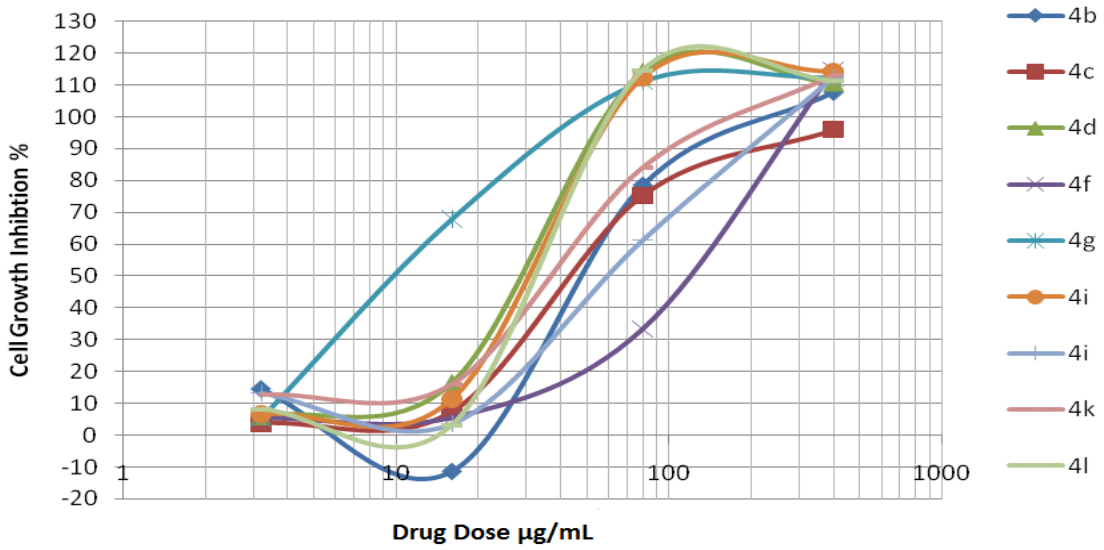

Figure 2 — Colon Cancer Cell (HCT116) growth inhibition against compounds **4b-l**

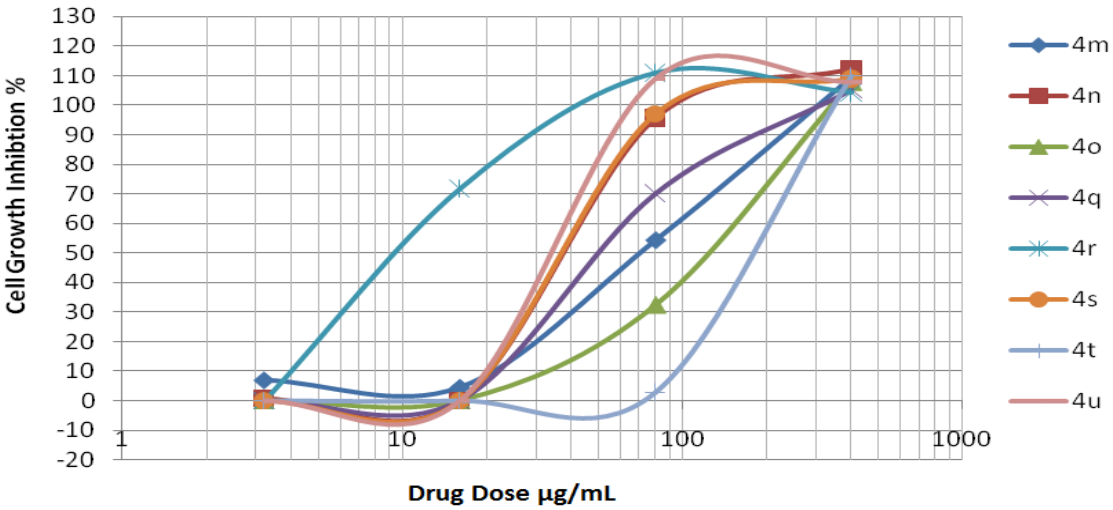

Figure 3 — Colon Cancer Cell (HCT116) growth inhibition against compounds **4m-u**

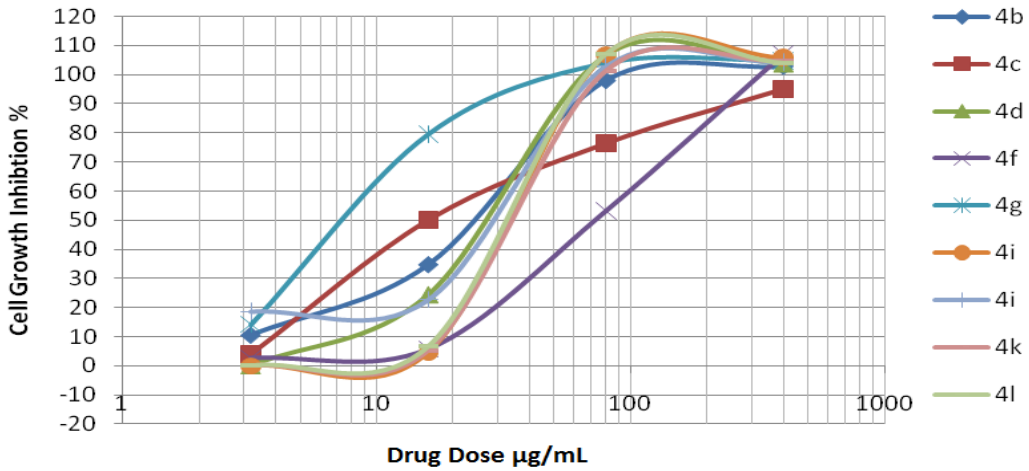

Figure 4 — Colon Cancer Cell (H1299) growth inhibition against compounds **4b-l**

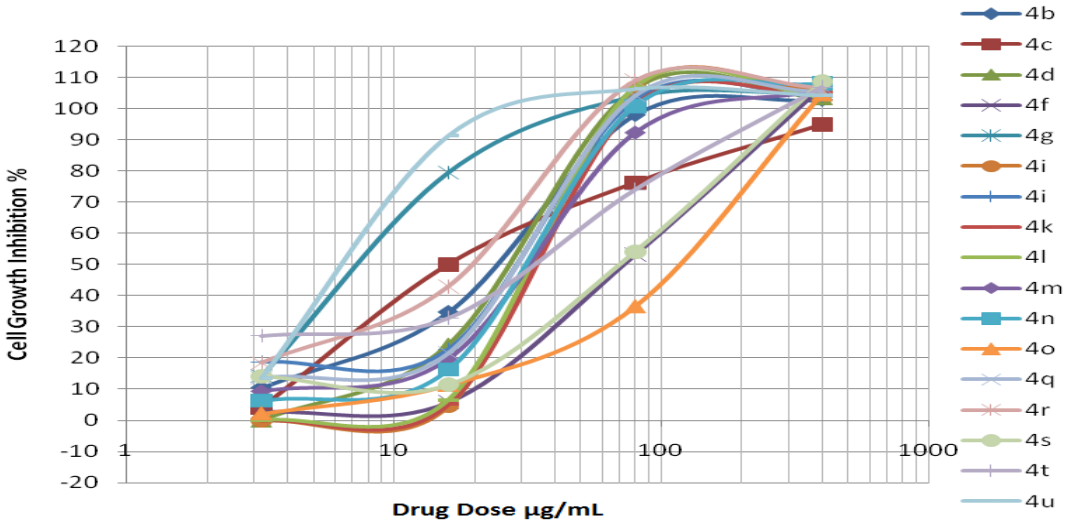

Figure 5 — Colon Cancer Cell (H1299) growth inhibition against compounds **4b-u**

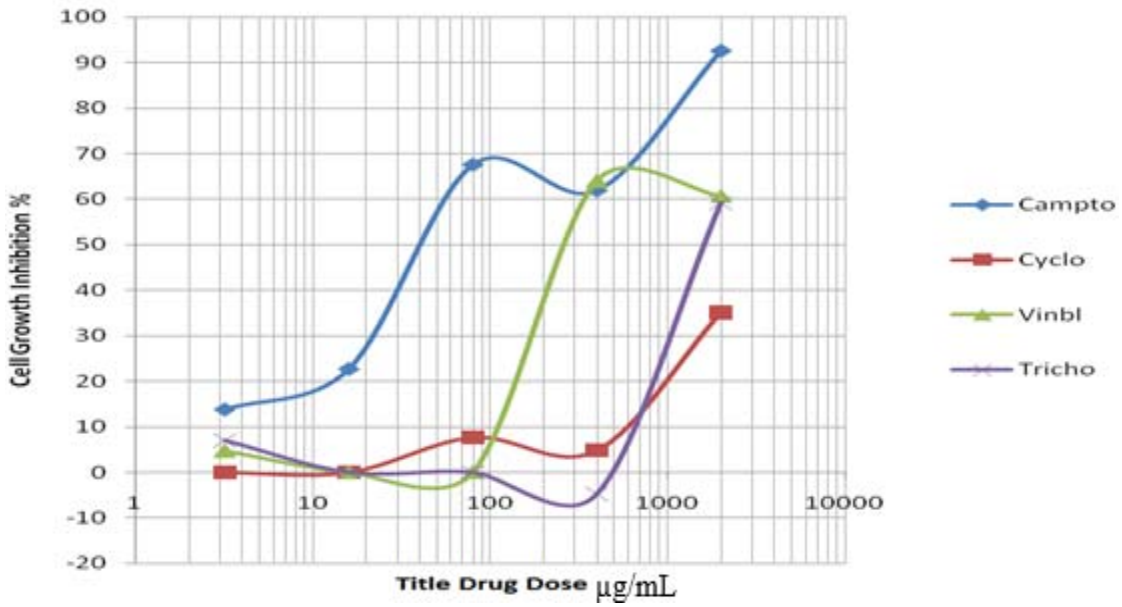

Figure 6 — Colon Cancer Cell (HCT116) growth inhibition against standard anticancer drugs

Table II — IC_{50} µg/mL of all synthesized compounds **4b-u**

	4b	**4c**	**4d**	**4f**	**4g**	**4i**	**4j**	**4k**	**4l**	**4m**	**4n**	**4o**	**4q**	**4r**	**4s**	**4t**	**4u**
HCT116	50	50	30	120	10	30	70	40	30	60	40	150	50	10	40	200	35
H1299	25	20	40	80	8	30	40	40	30	30	35	150	30	20	70	35	5.5

Table III — Docking score (kcal/mole) of various anticancer drugs with APOBEC3B (PDB ID: 5QCD)

S. No.	Ligand	Docking score (kcal/mole)
1.	Camptothecin	- 5.9
2.	Acyclovir	- 4.9
3.	Cisplatin	- 2.8
4.	Trichothecin	- 4.8
5.	Vinblastine	- 7.0

In order to achieve better insight into the molecular structure of the most bioactive stereoisomer or tautomeric forms for compounds **4a-u**, conformational analysis of the target compounds has been proposed (Figure 8).

The tautomeric equilibrium clearly reveals that the central amino residue is in interaction with the keto group of cyclohexanone moiety. So, a significant impact on the binding energies and binding process

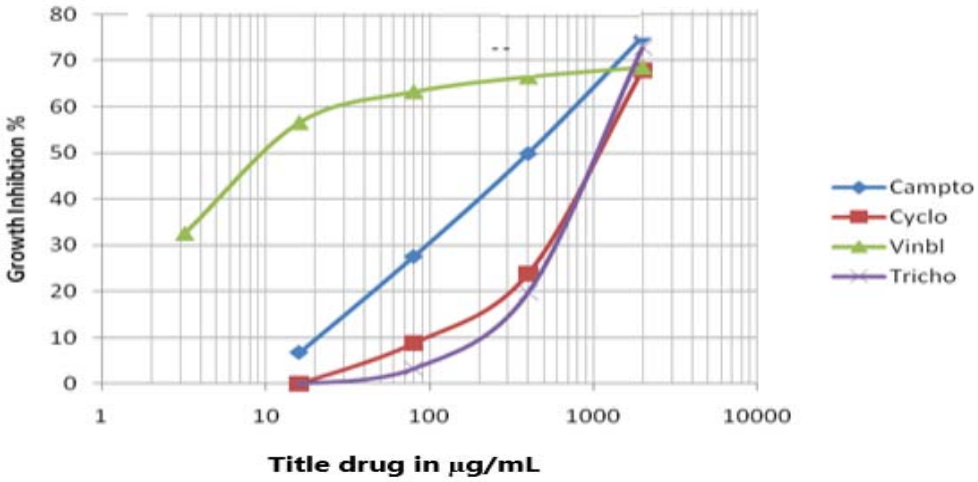

Figure 7 — Colon Cancer Cell (H1299) growth inhibition against standard anticancer drugs

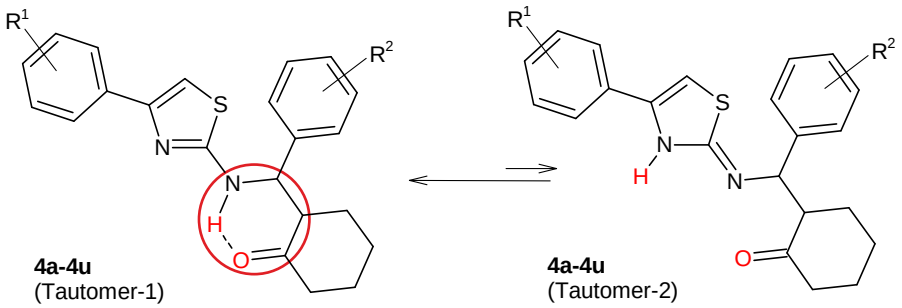

Figure 8 — Proposed tautomer structures of most stable stereoisomer compound

interaction with bio target were observed (Table II). This could probably be due to the presence of opening/closing pseudo-ring in the synthesized compounds **4a-u**.

Molecular modelling

Docking of the known anticancer drug in the active site of APOBEC3B (PDB ID: 5QCD) enzyme

A comparative study involving the interaction of known anticancer *viz*. Camptothecin, Acyclovir, Cisplatin, Trichothecin, and Vinblastine ion the active site pocket of APOBEC3B made for a better understanding of there anticancer action. Docking score of these depicted in Table III

In the case of APOBEC3B selective Vinblastine (Figure 9), the negative binding energies (-7.0 kcal/mol) are in agreement with its APOBEC3B selectivity as reported in several kinds of literature. Binding of Vinblastine in the binding pocket of APOBEC3B resulted from the conformational placement of amino acid residues in the active site and through hydrophobic interactions.

There is a weak hydrogen bond of 2.88, 3.18, 3.19, and 3.22Å between the vinblastine carbonyl and three amino acid *viz*. Arg212, Trp281, and Gln213, as well as they, show hydrophobic interaction. The distal carbonyl oxygen and carbon of vinblastine show aromatic as well as allyl interaction with Tyr215, Arg211, and Phe237.

Complexation of the docked ligand **4a-u** and standard drugs with APOBEC3B enzyme was interpreted by looking at the H-bonding or hydrophobic interaction of the ligand with the amino acid residues in the active site. The results are summarized in Table IV.

Docking of the synthesized ligand into APOBEC3B (PDB ID: 5CQD) active site

All the twenty-one synthesized β-amino carbonyl derivatives showed binding in the 5CQD active site with binding scores between -5.8 and -6.6 kcal/mol, as shown in Table IV. The compelling data can be utilized further to develop potent anti-cancer heterocycles.

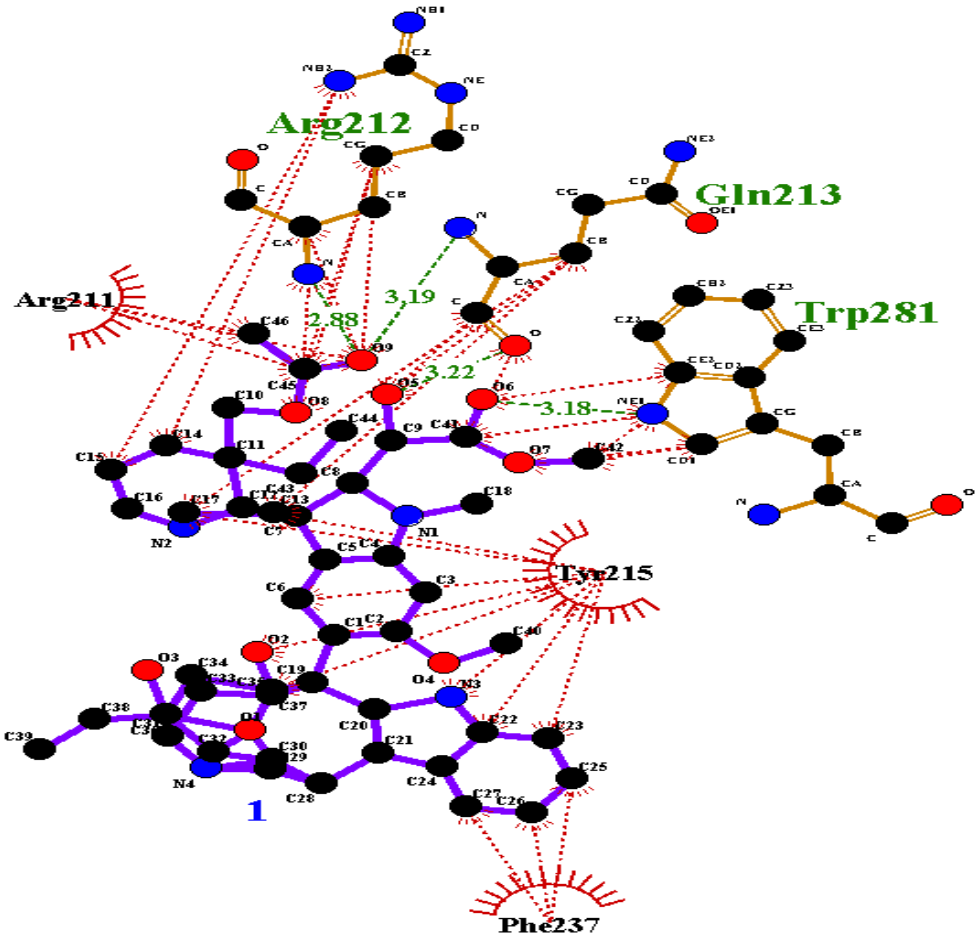

Figure 9 — LIGPLOT Ligand (Vinblastine)-protein PDB ID- 5CQD interaction diagram

Table IV — Docking score (kcal/mole) of different β-amino carbonyl analogue ligands **4a-u** with APOBEC3B (PDB ID: 5CQD)

S. No.	Ligand	Docking score (kcal/mol)	S. No.	Ligand	Docking score (kcal/mol)
1.	**4a**	-5.8	12.	**4l**	-5.9
2.	**4b**	-5.9	13.	**4m**	-5.9
3.	**4c**	-5.9	14.	**4n**	-6.2
4.	**4d**	-6.0	15.	**4o**	-6.1
5.	**4e**	-5.9	16.	**4p**	-5.9
6.	**4f**	-5.9	17.	**4q**	-6.3
7.	**4g**	-6.2	18.	**4r**	-6.4
8.	**4h**	-5.8	19.	**4s**	-6.5
9.	**4i**	-6.0	20.	**4t**	-6.6
10.	**4j**	-5.9	21.	**4u**	-6.3
11.	**4k**	-6.0			

Detailed 4t-5CQD structural interaction having the highest binding score among the other synthesized β-amino carbonyl derivatives

From a consideration of the stereo view of **4t** complexed inside the active-site gorge of 5CQD together with the LIGPLOT diagrams displayed in Figure 10, the following assignments can be made for protein-inhibitor interactions.

The carbonyl oxygen of Gln213 shows hydrophobic interaction with the sulfur and carbon atoms of the thiazole ring along with this sulfur from thiazole interact with the aromatic ring of Tyr215. On top of communication, there is a weak hydrogen bond of 3.07Å between the carbonyl oxygen of the cyclohexanone chain with the primary amine of Gln213. Near the top of the gorge, the distal nitro group of **4t** makes interaction with Tyr215

and a herringbone interaction with Gln213. At the bottom of the canyon and side amino acid, there is an aromatic-aromatic interaction between the proximal phenyl ring of **4t** and Trp281 and the carbon and nitrogen atom of nitro-substituted aromatic carbon ring interact with Tyr215. The Arg211 and Arg212 show electrostatic interaction between the cationic *meta* carbon of nitrobenzene ring and cyclohexanone ring.

The LIGPLOT diagrams in Figure 10 show atoms-atoms contacts of ≤ 3.09Å made by the three inhibitors, *viz*. **4r**, **4s**, and **4t** having the highest negative value compare with the other amino-acid residues lining the active site. The inhibitors show hydrophobic interaction with nearby side chains, as shown in red dashed. The red circles and ellipses in each plot designate protein residue that are corresponding 3D positions to the residues in the plot. The hydrogen bond is shown as green dotted lines, while the spoked arcs signify residues making nonbonded contact with the ligand. The highlighted equivalent side-chain residue has red underly beneath

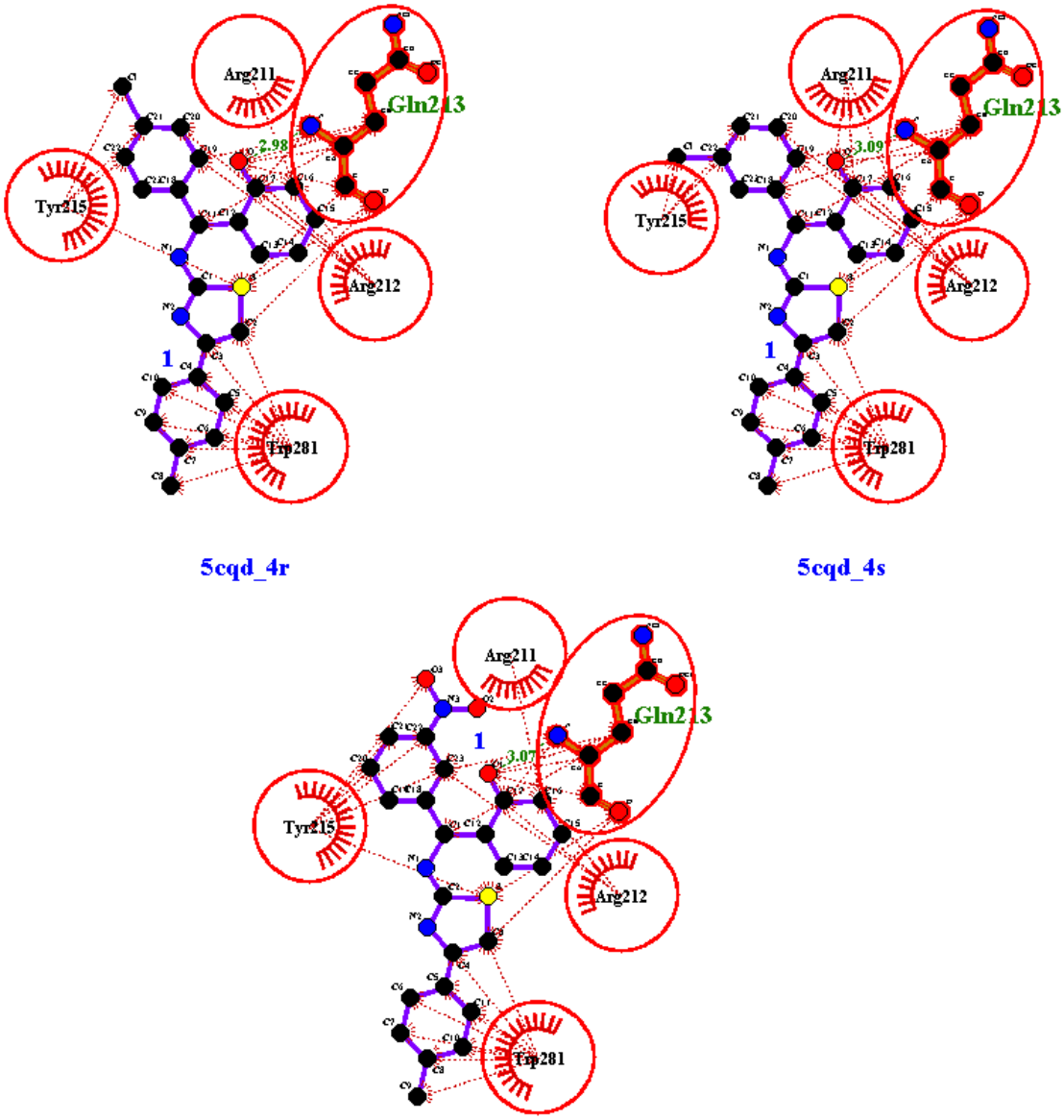

Figure 10 — Ligand-protein interaction diagrams for binding sites of the same protein APOBEC3B (PDB ID- 5CQD) each with a different ligand molecule having maximum negative binding value

there bond and atoms. Equivalent waste engaged in hydrophobic interaction shown in thicker lines.

Detailed study of Pharmacokinetics, Physicochemical, and Medicinal Properties by SwissADME online screening

The operational highlights of these molecules entered in the SwissADME site (http://swissadme.ch) utilizing the ChemAxon's Marvin JS structure drawing instrument. Auxiliary highlights of a pharmacophore impact the conduct of a unit in people, including bioavailability, transport properties, empathy to proteins, reactivity, poisonous quality, and metabolic steadiness. Incomparable to swissADME is the bioavailability radar [51] that gives a graphical preview of the medication similarity parameters of an orally available bioactive drug. The drug resemblance diagram displayed as a hexagon (Figure 11) with each of the vertices speaking to a setting that characterizes a bioavailable drug. The pink region inside the

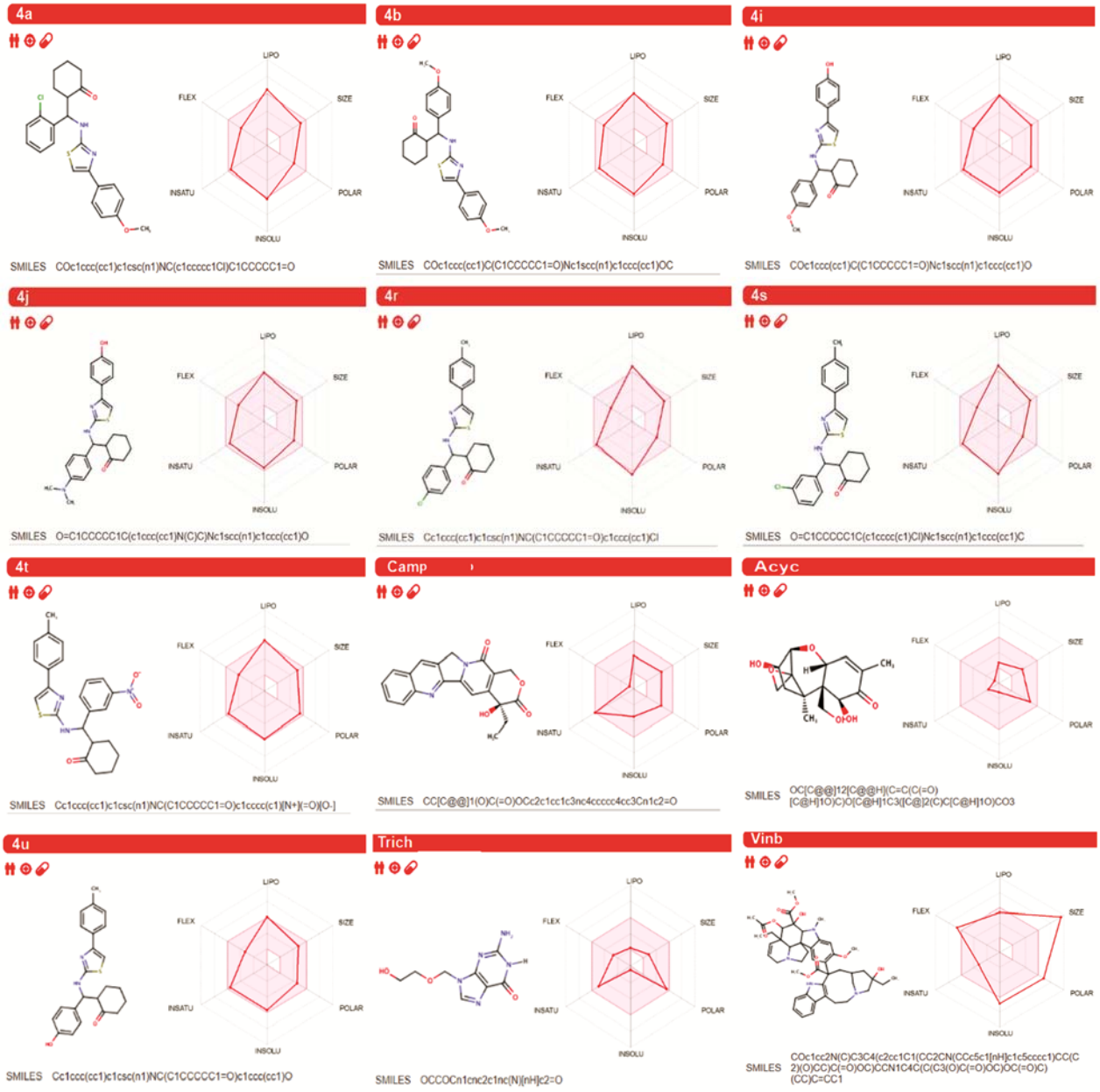

Figure 11 — The bioavailability radar of the synthesized molecules (**4a-u**) and standard drugs (Camp., Acyc., Trich., Vinb.) evaluating using the swissADME web tool

hexagon speaks to the ideal range for every property (lipophilicity: XLOGP3 between − 0.7 and + 5.0, size: polarity: TPSA somewhere in the range of 20 and 130 Å, MW somewhere in the range of 150 and 500 g/mol, solubility: log S not higher than 6, flexibility: close to 9 rotatable bonds, and saturation: part of carbons in the sp3 hybridization at least 0.25) Table V.

Drug-likeness

The drug resemblance properties of the fused compound and standard drug are articulated to by the red mutilated hexagon inside the pink shade (Figure 11). The **4b-d**,**g-k**,**n-p**,**t-u** molecules fall within the drug-likeness parameter of a bioavailable drug. While **4a**,**r**,**s** shows outside parameters describe for lipophilicity and insolubility for bioavailability parameter and **4e**,**f**,**l**,**m** have slightly outside the optical range of lipophilicity. (Figure 11). SwissADME likewise has computational channels that incorporate Ghose[52], Egan[53], Veber[54], and Muegee[55] created by top pharmaceutical organizations and cheminfomaticians to assess the drug resemblance of molecules.

The Ghose screen quantitatively describes molecules dependent on figured physicochemical property profiles that incorporate log P, molar refractivity (MR), molecular weight (MW), and several atoms. The passing scope of determined log P (ClogP) is between -0.4 and 5.6. For MW, the moving extent is somewhere in the range of 160 and 480. For MR, the passing reach is somewhere in the range of 40 and 130, and for the total number of atoms, the moving extent is between 20 and 70 atoms in a small molecule. Our compounds **4b,c, g-q, t-u**, and out of four standard drugs tested only camptothecin qualify the Ghose qualifying criteria, but the molecule **4a,e,f,r**, and **4s** out of the qualifying range (Table VI).

Veber (GSK filter) model represents molecules as druglike on the off chance that they have ten or less rotatable bonds and a PSA equivalent to or under 140 Å2 with 12 or less H-bond donors and acceptors.

Egan (Pharmacia) filter gives an expectation of drug assimilation dependent on physical procedures engaged with film absorbency of a molecule. Significantly, the Egan computational model for human passive intestinal absorption (HIA) of

Table V — Physicochemical properties of the synthesized molecules **(4 a-u)** and standard drugs(MW: Molecular weight; HA: Heavy atoms; AHA: Aromatic heavy atom; FCsp3: Fraction Csp3; RTB: Rotatable bonds; HBA: H-bond acceptors; HBD: H-bond donors; MR: Molar refractivity; TPSA: Total polar surface area).

Sr. No.	MW	HA	AHA	FCsp3	RTB	HBA	HBD	MR	TPSA
4a	426.96	29	17	0.3	6	3	1	119.77	79.46
4b	422.54	30	17	0.33	7	4	1	121.25	88.69
4c	435.58	31	17	0.36	7	3	1	128.97	82.7
4d	410.5	29	17	0.3	6	4	1	114.72	79.46
4e	426.96	29	17	0.3	6	3	1	119.77	79.46
4f	426.96	29	17	0.3	6	3	1	119.77	79.46
4g	437.51	31	17	0.3	7	5	1	123.58	125.28
4h	392.51	28	17	0.3	6	3	1	114.76	79.46
4i	408.51	29	17	0.3	6	4	2	116.79	99.69
4j	421.56	30	17	0.33	6	3	2	124.5	93.7
4k	396.48	28	17	0.27	5	4	2	110.25	90.46
4l	412.93	28	17	0.27	5	3	2	115.3	90.46
4m	412.93	28	17	0.27	5	3	2	115.3	90.46
4n	423.48	30	17	0.27	6	5	2	119.12	136.28
4o	394.49	28	17	0.27	5	4	3	112.32	110.69
4p	378.49	27	17	0.27	5	3	2	110.29	90.46
4q	406.54	29	17	0.33	6	3	1	119.73	79.46
4r	410.96	28	17	0.3	5	2	1	118.25	70.23
4s	410.96	28	17	0.3	5	2	1	118.25	70.23
4t	421.51	30	17	0.3	6	4	1	122.06	116.05
4u	392.51	28	17	0.3	5	3	2	115.26	90.46
Camp	348.35	26	16	0.25	1	5	1	95.31	81.42
Acyc	296.32	21	0	0.8	1	6	3	70.66	99.52
Trich	225.2	16	9	0.38	4	5	3	55.68	119.05
Vinb	810.97	59	15	0.59	10	11	3	232.52	154.1

molecule represents dynamic carriage and efflux components and is, in this way, vigorous in foreseeing adaptation of drugs. The Egan violation only observed in **4n**,**r**,**s**, and standard vinblastine drugs (Table VI).

Muegge (Bayer filter) model is a database-free pharmacophore point screen that separates between drug-like and nondrug-like matter. It depends on the perception that non-drugs are frequently less functionalized. Four purposeful themes are characterized to be significant in drug-like molecules and incorporate hydroxyl, amine, ketone, and sulfonyl groups. In this manner, a base check of well-characterized pharmacophore focuses is required to pass the screen. The manifestation of these efficient themes ensures hydrogen-holding capacities that are basic for explicit drug cooperation with its objectives. These serviceable groups can consolidate to what Muegge model alludes to as pharmacophore points. The pharmacophore emphases incorporate amine, amide, alcohol, ketone, sulfone, sulfonamide, carboxylic acid, carbamate, guanidine, amidine, urea, and active ester groups. These pharmacophore efforts in molecules possibly give critical communications with the objective protein. From the screening data, the synthesized compound **4a-h**,**l**,**m**,**q**,**r**,**s**,**t**, and **u** that they don't have the recommended functional group for the interaction with the target protein suggested by the Muegge.

PAINS, Break and Leadlikeness screening

PAINS (pan-assay interference screening) that often gives false favourable chemical properties results in high-throughput screens. PAINS tend to react non-specifically with numerous biological targets rather than specifically affecting one anticipated goal.

PAINS (pan-assay interference screening) that regularly give false favourable synthetic properties bring about high-throughput screens. PAINS will, in general, respond non-specifically with various biological targets as opposed to explicitly influencing one anticipated objective. SwissADME evaluation did not post any PAINS alert except **4c** and **4j** molecules (Table VII).

In another choice model, Brenk[56] considered composites that are smaller and less hydrophobic and

Table VI — Drug-likeness evaluation of synthesized compounds (**4 a-u**) using swissADME

Sr. No.	Lipinski #violations	Ghose #violations	Veber #violations	Egan #violations	Muegge #violations
4a	0	1	0	0	1
4b	0	0	0	0	1
4c	0	0	0	0	1
4d	0	1	0	0	1
4e	0	1	0	0	1
4f	0	1	0	0	1
4g	0	0	0	0	1
4h	0	0	0	0	1
4i	0	0	0	0	0
4j	0	0	0	0	0
4k	0	0	0	0	0
4l	0	0	0	0	1
4m	0	0	0	0	1
4n	0	0	0	1	0
4o	0	0	0	0	0
4p	0	0	0	0	0
4q	0	0	0	0	1
4r	0	1	0	1	1
4s	0	1	0	1	1
4t	0	0	0	0	1
4u	0	0	0	0	1
Camp	0	0	0	0	0
Acyc	0	1	0	0	0
Trich	0	1	0	0	0
Vinb	2	3	1	1	4

Table VII — Medicinal chemistry evaluation of the synthesized compounds

Sr. No.	PAINS #alerts	Brenk #alerts	Leadlikeness #violations	Synthetic Accessibility
4a	0	0	2	3.97
4b	0	0	2	4.01
4c	2	0	2	4.13
4d	0	0	2	3.89
4e	0	0	2	3.87
4f	0	0	2	3.91
4g	0	2	2	4.06
4h	0	0	2	3.86
4i	0	0	2	3.9
4j	2	0	2	4.03
4k	0	0	2	3.79
4l	0	0	2	3.78
4m	0	0	2	3.82
4n	0	2	2	3.97
4o	0	0	2	3.81
4p	0	0	2	3.77
4q	0	0	2	3.98
4r	0	0	2	3.93
4s	0	0	2	3.96
4t	0	2	2	4.11
4u	0	0	2	3.89
Camp	0	0	0	3.84
Acyc	0	1	0	5.42
Trich	0	0	1	2.47
Vinb	0	2	3	9.65

not those characterized by "Lipinski's standard of 5" to enlarge open doors for lead streamlining. That was after the prohibition of compounds with possibly mutagenic, reactive, and unfavourable groups, for example, nitro, sulfates, phosphates, 2-halopyridines, and thiols. Brenk model confines the ClogP/ClogD to sandwiched between zero and four, the quantity of hydrogen-bond donors and acceptors to less than 4 and 7, individually, and the number of substantial atoms to in the range of 10 and 27. Furthermore, just compounds with restricted entanglement characterized as less than eight rotatable bonds, less than five ring structures, and no ring structures with more than two fused rings are considered medicinal. The **4g**,**n**, and **4t** flouted two break rules by the presence of one nitro group, and standard Vinblastine also had two breaks.

Leadlikeness tests are proposed to furnish leads with great kinship in high-throughput screens that take into account the detection and manipulation of new exchanges in the lead advancement stage (Table VII). The standard drugs camptothecin and acyclovir passed all the leadlikness criteria, while the synthesized compound with the standard trichothecene and vinblastine fail in leadlikness.

P-glycoprotein and CYP enzyme activity prediction

SwissADME additionally empowers the estimation for a compound to be a substrate of p-glycoprotein (P-gp) or inhibitor of the cytochrome p450 isoenzymes (CYP isoenzymes). P-gp is broadly dispersed and communicated in the intestinal epithelium where it thrusts xenobiotics, for example, medicates over into the intestinal lumen and in the delicate endothelial cells making the blood-brain barrier where it propels them once again into the vessels. CYP isoenzymes are in charge of the biotransformation of drugs[57]. Drug digestion through CYP isoenzymes is a significant determinant of drug connections that can prompt to drug toxicities and diminished pharmacological impact. The models return "Yes" or "No" if the molecule under examination has a higher likelihood to be substrate or non-substrate of P-gp or inhibitor or non-inhibitor of a given CYP. The screening results are tabulated in Table VIII.

Table VIII — Pharmacokinetic evaluation of the synthesized compounds (GI: gastro-intestinal absorption; BBB: blood-brain barrier; CYP: Cytochromes, P-gp: P-glycoprotein)

Sr. No.	GI absorption	BBB permeant	Pgp substrate	CYP1A2 inhibitor	CYP2C19 inhibitor	CYP2C9 inhibitor	CYP2D6 inhibitor	CYP3A4 inhibitor
4a	High	No	Yes	No	Yes	Yes	Yes	Yes
4b	High	No	Yes	No	Yes	Yes	Yes	Yes
4c	High	No	Yes	No	Yes	Yes	Yes	Yes
4d	High	No	Yes	No	Yes	Yes	Yes	Yes
4e	High	No	Yes	No	Yes	Yes	Yes	Yes
4f	High	No	Yes	No	Yes	Yes	Yes	Yes
4g	Low	No	No	No	Yes	Yes	No	Yes
4h	High	No	Yes	Yes	Yes	Yes	Yes	Yes
4i	High	No	Yes	Yes	Yes	Yes	Yes	Yes
4j	High	No	Yes	Yes	Yes	Yes	Yes	Yes
4k	High	No	Yes	Yes	Yes	Yes	Yes	Yes
4l	High	No	Yes	Yes	Yes	Yes	Yes	Yes
4m	High	No	Yes	Yes	Yes	Yes	No	Yes
4n	Low	No	Yes	Yes	Yes	Yes	No	Yes
4o	High	No	Yes	Yes	Yes	Yes	Yes	Yes
4p	High	No	Yes	Yes	Yes	Yes	Yes	Yes
4q	High	No	Yes	No	Yes	Yes	Yes	Yes
4r	High	No	Yes	Yes	Yes	Yes	No	Yes
4s	High	No	Yes	Yes	Yes	Yes	No	Yes
4t	Low	No	No	Yes	Yes	Yes	No	Yes
4u	High	No	Yes	Yes	Yes	Yes	Yes	Yes
Camp	High	No	Yes	Yes	No	Yes	No	Yes
Acyc	High	No	Yes	No	No	No	No	No
Trich	High	No	No	No	No	No	No	No
Vinb	Low	No	Yes	No	No	No	No	Yes

HIA and BBB prediction

Appropriate to P-gp and CYP protein energy is human gastrointestinal ingestion (HIA) and blood-brain barrier infiltration (BBB). SwissADME 'BOILED-Egg' (Figure 12) permits for assessment of HIA as an element of the situation of the molecules in the WLOGP-*versus*-TPSA referential. The white section of the 'BOILED-Egg' is for a high possibility of reflexive adaptation by the gastrointestinal tract, and the yellow area (yolk) is for a high probability of cerebrum entrance. Yolk and white zones are not fundamentally unrelated. With this, the points are shaded in blue whenever anticipated as effectively effluxed by P-gp (PGP+) and in red projected as non-substrate of P-gp (PGP−). All the synthesized compound shows high GI absorption and no BBB prediction except **4g**,**t** (red dot) and **4n** they have the low GI and no BBB prediction. (Figure 12).

HIA and BBB are subject to water solubility and lipophilicity of the drug. Two topological approaches to foresee water solubility comprised of SwissADME. The first is an execution of the ESOL[58] model, and the subsequent one modified from Ali *et al*.[59]. Swiss ADME third indicator for solubility was created by SILICON-IT. All anticipated qualities are the decimal logarithm of the molar solubility in water (log S).

The Ali and Silicoms IT screening show poor solubility of all the synthesized compound while in ESOL solubility analysis most of the compounds are moderately soluble except **4a**,**f**,**r** and **s** they show poor solubility (Table IX). Even the standard drugs are in the range of poor solubility to very soluble. Consensus Log p is the average value of all Log P evaluated with various lipophilicity criteria (Table X).

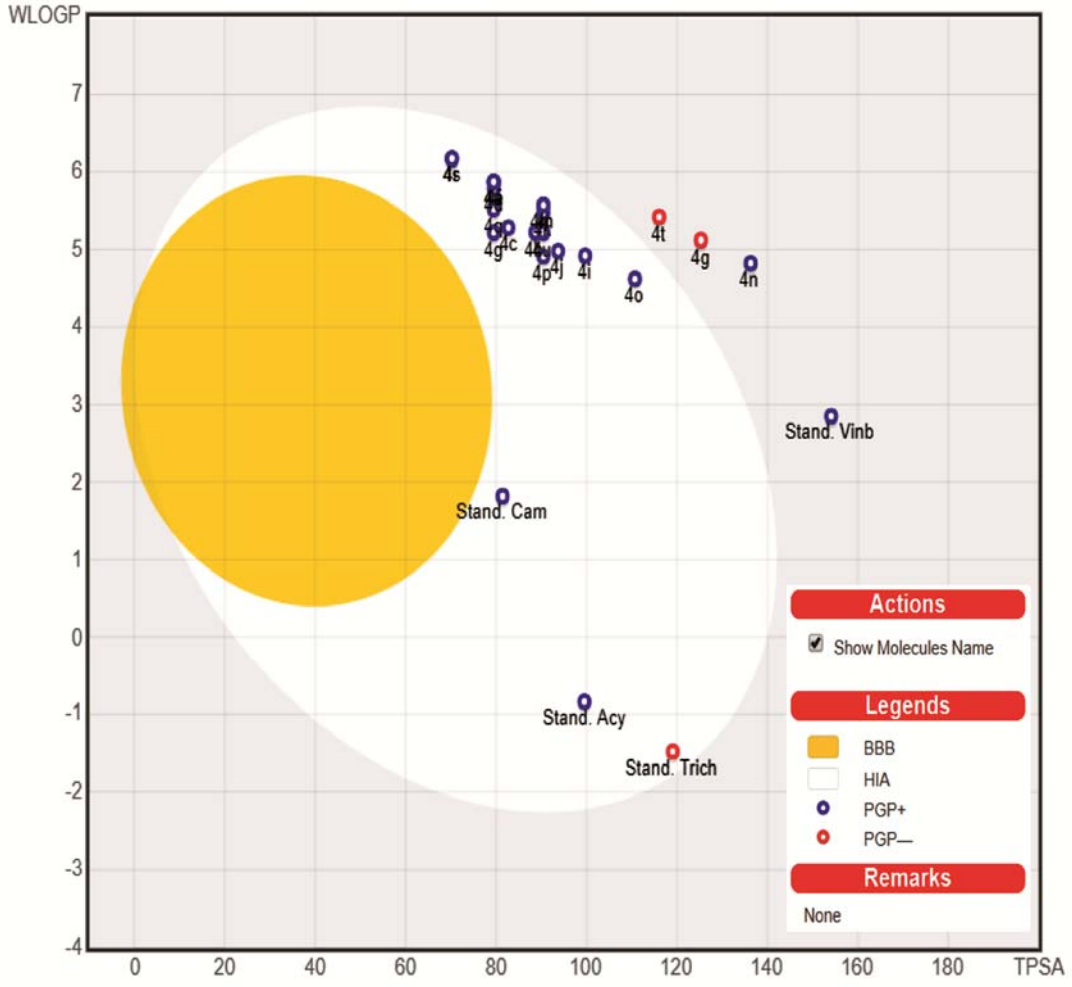

Figure 12 — The BOILED-Egg allows for evaluation of passive gastrointestinal absorption (HIA), brain penetration (BBB) and P-glycoprotein in the presence of the molecule (P-gp)

Table IX — Water solubility evaluation of the synthesized compounds (Solu.: Solubility; PS: Poorly soluble; MS: Moderately soluble; S: soluble; VS: Very soluble)

Sr. No.	ESOL				Ali				Silicon-IT			
	Log S	Solu. (mg/mL)	Solu. (mol/L)	Class	Log S	Solu. (mg/mL)	Solu. (mol/L)	Class	LogSw	Solu. (mg/mL)	Solu. (mol/L)	class
4a	-6.18	2.83E-04	6.62E-07	PS	-7.24	2.47E-05	5.77E-08	PS	-8.39	1.72E-06	4.03E-09	PS
4b	-5.66	9.21E-04	2.18E-06	MS	-6.76	7.38E-05	1.75E-07	PS	-7.91	5.19E-06	1.23E-08	PS
4c	-5.82	6.54E-04	1.50E-06	MS	-6.79	7.10E-05	1.63E-07	PS	-7.88	5.72E-06	1.31E-08	PS
4d	-5.75	7.31E-04	1.78E-06	MS	-6.7	8.21E-05	2.00E-07	PS	-8.07	3.47E-06	8.45E-09	PS
4e	-6.18	2.83E-04	6.62E-07	PS	-7.24	2.47E-05	5.77E-08	PS	-8.39	1.72E-06	4.03E-09	PS
4f	-6.18	2.83E-04	6.62E-07	PS	-7.24	2.47E-05	5.77E-08	PS	-8.39	1.72E-06	4.03E-09	PS
4g	-5.65	9.73E-04	2.22E-06	MS	-7.38	1.82E-05	4.16E-08	PS	-7.15	3.10E-05	7.10E-08	PS
4h	-5.59	1.01E-03	2.57E-06	MS	-6.6	9.97E-05	2.54E-07	PS	-7.81	6.09E-06	1.55E-08	PS
4i	-5.45	1.46E-03	3.57E-06	MS	-6.65	9.22E-05	2.26E-07	PS	-7.22	2.46E-05	6.01E-08	PS
4j	-5.61	1.04E-03	2.47E-06	MS	-6.68	8.88E-05	2.11E-07	PS	-7.19	2.71E-05	6.43E-08	PS
4k	-5.54	1.15E-03	2.91E-06	MS	-6.59	1.03E-04	2.59E-07	PS	-7.38	1.64E-05	4.14E-08	PS
4l	-5.97	4.41E-04	1.07E-06	MS	-7.14	3.01E-05	7.29E-08	PS	-7.71	8.14E-06	1.97E-08	PS
4m	-5.97	4.41E-04	1.07E-06	MS	-7.14	3.01E-05	7.29E-08	PS	-7.71	8.14E-06	1.97E-08	PS
4n	-5.44	1.55E-03	3.65E-06	MS	-7.27	2.28E-05	5.38E-08	PS	-6.46	1.47E-04	3.48E-07	PS
4o	-5.24	2.27E-03	5.75E-06	MS	-6.55	1.12E-04	2.85E-07	PS	-6.53	1.16E-04	2.95E-07	PS
4p	-5.38	1.58E-03	4.19E-06	MS	-6.48	1.24E-04	3.28E-07	PS	-7.12	2.88E-05	7.62E-08	PS
4q	-5.89	5.25E-04	1.29E-06	MS	-6.97	4.37E-05	1.07E-07	PS	-8.19	2.66E-06	6.53E-09	PS
4r	-6.41	1.59E-04	3.86E-07	PS	-7.46	1.43E-05	3.47E-08	PS	-8.67	8.81E-07	2.14E-09	PS
4s	-6.41	1.59E-04	3.86E-07	PS	-7.46	1.43E-05	3.47E-08	PS	-8.67	8.81E-07	2.14E-09	PS
4t	-5.88	5.57E-04	1.32E-06	MS	-7.59	1.08E-05	2.56E-08	PS	-7.42	1.59E-05	3.78E-08	PS
4u	-5.68	8.29E-04	2.11E-06	MS	-6.86	5.45E-05	1.39E-07	PS	-7.49	1.26E-05	3.21E-08	PS
Camp	-3.49	1.14E-01	3.27E-04	S	-3.07	2.99E-01	8.58E-04	S	-5.83	5.20E-04	1.49E-06	MS
Acyc	-1.16	2.06E+01	6.96E-02	VS	-0.89	3.78E+01	1.28E-01	VS	-0.81	4.59E+01	1.55E-01	S
Trich	-0.41	8.85E+01	3.93E-01	VS	-0.43	8.32E+01	3.69E-01	VS	-1.28	1.19E+01	5.28E-02	S
Vinb	-6.84	1.17E-04	1.44E-07	PS	-6.81	1.25E-04	1.54E-07	PS	-8.46	2.80E-06	3.45E-09	PS

Experimental Section

Every one of the reactions was conveyed under the stipulated conditions, utilizing freshly prepared thiazole, ionic liquid, and pure solvents. The open capillary technique was utilized to decide the dissolving purpose of the compound and are uncorrected. The refined dissolvable was utilized to perform TLC on silica gel G. All the synthetic compounds were bought from S.D. Fine synthetic substances of AR grade. ^{1}H NMR and ^{13}C NMR spectra recorded from DMSO-d_6 arrangements on a Brucker AC 400 (MHz). TMS as an inward standard for detailing the substance move in ^{1}H NMR. KBr plates strategy used to IR spectra on a Perkin Elmer 1800 spectrophotometer and mass spectra interpretation finished with a GC-MS (70ev). All tertiary alkyl amines concentrated H_2SO_4, cyclohexanone, and aromatic aldehydes obtained from S.D. Fine chemicals of AR grades.

Procedure for 2-amino-4-(4-methoxyphenyl) thiazole2a[49]

The title compound was set up by the expansion of resublimed iodine (0.01 moles) to 1-(4-methoxyacetophenone (0.01 mol) and thiourea (0.02 mol), trailed by warming of the blend on a water bath at 100°C. The cooled reaction mixture was triturated with diethyl ether to evacuate any unreacted iodine and acetophenone. The solid residue was placed in cold water (250 mL) and treated with aqueous ammonium hydroxide. The precipitated thiazole was gathered and cleansed by crystallization from ethanol. The yield was 88%.

General procedure for preparation of rac-(2S)-2-[(R)-[(4-substituted phenyl){[4-(4-substitutedphenyl) - 1,3-thiazol-2-yl]amino}methyl]cyclohexanone(4a-4u)[17]

The preparation of substituted β-amino carbonyl derivatives investigated in several ionic liquids. The

Table X — lipophilicity evaluation of the synthesized compounds

Sr. No.	iLOGP	XLOGP3	WLOGP	MLOGP	Silicos-IT Log P	Consensus Log P
4a	3.67	5.8	5.87	3.54	6.45	5.07
4b	3.67	5.15	5.22	2.71	5.88	4.53
4c	3.85	5.3	5.28	2.92	5.5	4.57
4d	3.68	5.28	5.78	3.44	6.24	4.88
4e	3.82	5.8	5.87	3.54	6.45	5.1
4f	3.74	5.8	5.87	3.54	6.45	5.08
4g	3.32	5.01	5.12	2.1	3.65	3.84
4h	3.65	5.18	5.22	3.06	5.82	4.59
4i	3.28	4.82	4.92	2.5	5.33	4.17
4j	3.25	4.97	4.98	2.71	4.96	4.17
4k	3.2	4.95	5.47	3.23	5.7	4.51
4l	3.11	5.48	5.57	3.33	5.92	4.68
4m	3.3	5.48	5.57	3.33	5.92	4.72
4n	2.75	4.68	4.82	1.89	3.1	3.45
4o	2.82	4.5	4.62	2.29	4.8	3.81
4p	3.02	4.85	4.91	2.85	5.29	4.18
4q	3.96	5.54	5.52	3.28	6.34	4.93
4r	4.01	6.2	6.17	4.13	6.92	5.49
4s	3.95	6.2	6.17	4.13	6.92	5.47
4t	3.23	5.4	5.42	2.63	4.11	4.16
4u	3.14	5.21	5.22	3.06	5.8	4.49
Cam	2.49	1.74	1.82	1.64	3.29	2.2
Acy	1.78	-0.72	-0.84	-0.74	0.8	0.06
Tric	0.48	-1.56	-1.48	-1.43	-0.57	-0.91
Vin	5.06	3.88	2.85	2.35	4.72	3.77

choices of ionic liquids were motivated by there being the most widely used, and therefore the most widely available[50].

Biological Assay

In vitro anticancer assays

In this assay, the viability of chemically treated cells measured by a dye, Resazurin, or Alamar blue (AB). AB, a non-fluorescent marker colour, is changed over to brilliant red– fluorescent resorufin employing the reduction reactions of metabolically dynamic cells. The quantity of living cells is legitimately corresponding to the measure of fluorescence delivered.

Protocol:

1 Trypsinize the cell and dilute with RPMI medium (with 5% serum)
2 Count the cells and dilute them in the same RPMI medium.
3 Add 100,000 cells per well in 40 µL. Use 384 well black plates.
4 Make a 2X solution for each dilution in the RPMI medium and add 50µL per well. Use appropriate positive and negative controls.
5 Add 10 µL Alamar blue and incubate ON.
6 Measure Fluorescence. (560nm / 590 nm Ex/Em). The contrast in fluorescence intensity estimates the counter cancer impact of that compound.

Sample (5 mg) was dissolved in 250 µL DMSO to achieve a concentration of 20 mg/mL. In each well, 100 µL medium with cells was added and allowed to grow overnight so that cells attained a limit of 10.000 cells / well. Two cell lines HCT116 (Mismatched DNA repair deficiency) and H1299 (P53 deficient). The supernatant medium discarded, and 100 µL of fresh medium added. The top of the well had 125 µL of the solution; 2.5 µL of stock solution added. The net concentration of the cells was 400 µg/mL. The material was inserted into the second row of the microtiter plates and sequentially diluted to 1/5: a total of six dilutions made. The 7^{th} and 8^{th} rows used as controls. The plates incubated for 48 hours, and the supernatant discarded. Fresh medium containing 2% Alomar Blue added. Further incubation of 2 hours was followed by a reading of the fluorescence intensity. The active cells released the fluorescence; the intensity was directly proportional to the number

of cells. Both HCT116 and H1299 are colon cancer cell lines obtained from ATCC. HCT116 is a mismatch repair-deficient cell line, and H1299 has a p53 mutation.

In vitro anti-cancer activity

Standard Alamar Blue Assay protocol for Cell viability assay used. Coherently developed cells were trypsinized, and around 10,000 cells seeded in each well of 96 well plates. The next day the medium was supplanted with medium containing suitable centralization of the drug. Compounds were suspended in 250 µL DMSO, and 2.5 µL added to each well in 125 µL, 1/5 dilution up to 5 dilutions for HCT116/H1299 Cancer cell line. The maximum concentration of each drug is 400 µg/mL, 1/5 dilution used for each drug. The cells treated for 48 hours and 2 µL of Alamar blue was added to each well and brooded for two hours. Fluorescence intensity read with a plate reader. The IC_{50} value was calculated from the graph.

Computational Details

All the ligand used was made using ChemDraw 3D [60]. Before the docking calculation of the ligands, the structure was lower in energy and then docked by using PyRx[61]. The crystal structure for the complex with an inhibitor downloaded from Protein Data Bank (http://www.rscb.org/) as a PDB file. The active site of the docked protein was found out by Argus Lab 4.0[62], which used for the docking in the PyRX.

The downloaded protein of the Cancer Genomic DNA Mutator APOBEC3B (PDB ID- 5CQD) contain chain A and C with Glycerin; Propane-1,2,3-triol and zinc ion as interacting ligand. The selected chain A contains 185 residues having twenty-six active site *viz*. Arg211, Arg212, Arg257, Asn240, Asp346, Cys239, Cys284, Cys289, Gln213, Glu241, Glu255, Glu342, His253, Leu238, Leu318, Met186, Phe237, Phe285, Pro283, Ser286, Thr214, Trp281, Trp287, Tyr191, Tyr215 and Tyr313. The chain A and C with the residues, water, and hetero group within a radius of 2.08A° refined for further cleaned by ascertaining the hybridization and introducing the H-atoms to the protein residue with the removal of water molecules. The cleaned structure of the Cancer Genomic DNA Mutator APOBEC3B (PDB ID- 5CQD) chain A carried no charge, 1356 valence electron, and 496 atoms. The docking with PyRx (Autodock) was conducted vina search space of dimension size x = 45.9667083596, y = 33.1205244125, z = 34.2302049496; center x = 73.3676401887, y = 4.22414666002, z = 0.401404471846 with nine exhaustiveness. The best conformational binding energy reported in Table VI. The LIGPLOT+ version V.1.4.5[63] was used to find the multiple ligand-protein interaction diagram.

Conclusion

All compounds were evaluated *in vitro* against a two-cell line panel consisting of HCT116 and H1299, respectively. Results indicate that all the substituted 2-((4-phenyl)(4-(4-phenyl)thiazol-2-ylamino)methyl) cyclohexanone derivatives **4a-u** are active.

From the graphical representation, it can conclude that the compounds **4b**,**c** and **q** moderate repressive while the **4j**,**m** weak inhibitory activity, and **4f**,**o** and **t** have very less action against but out of which **4g**, **r** shows proposing an operation against a cancer cell line HCT116. In case activity against H1299 cell lines,**4g** shows excellent activity while the others are moderate activity. The compound **4r**, **4s**, and **4t** show comparable binding energy score with the standard drug-like Vinblastine (-7.0kcal/mol) and higher as compare to Camptothecin (-5.9 kcal/mol).

Acknowledgements

We express our gratitude to SAIF, Chandigarh, for spectral analysis. We pay special thanks to Dr D. Palaniyandi Manivasakam, Director, Biology Indus Pharmaceuticals 25 Olympia Avenue Suite K-600, Woburn, MA 01801, for anticancer screening.

References

1 Brana M F & Migallon A S, *Clinical and Translational Oncology*, 8(10) (2006) 717.
2 Hieu B T, Thuy L T, Thuy V T, Tien H X & Chinh L V, *Bulletin Korean Chem Soc*, 33 (2012) 1586.
3 Gul H I, Yerdelen K O, Gul M, Das U & Pandit B, *Arch Pharm Chem Life Sci*, 340 (2007) 195.
4 Gul H I, Yerdelen K O, Gul M, Das U & Pandit B, *Chem Pharm Bull*, 56 (2008) 1675.
5 Dimmock J M, Kandepu N M, Hetherington M, Quail J W & Pugazhenthi U, *J Med Chem*, 41 (1998) 1014.
6 Karll R E & Lee R J, *US Patent*, US 4,384,138 (1983).
7 Otto F P, *US Patent*, US 3, 649,229 (1972).
8 Horodysky A G & Kaminski J M, *US Patent*, US4, 394, 278 (1983).
9 Scott M K, Martin G E, DiStefano D L, Fedde C L & Kukla M J, *J Med Chem*, 35 (1992) 552.
10 Cohen A, Hall R A, Heath-Brown B, Parkes M W & Rees A H, *British J Pharm Chemother*, 12 (1957) 194.

11 Borenstein M R & Doukas P H, *J Pharm Sci*, 76 (1987) 300.
12 Shiozawa A, Narita K, Izumi G, Kurashige S & Sakitama K, *Eur J Med Chem*, 30 (1995) 85.
13 Barlin G B & Jiravinja C, *Australian J Chem*, 43 (1990) 1175.
14 Barlin G B, Jiravinja C & Yan J H, *Australian J Chem*, 44 (1991) 677.
15 (a) Edwards M L, Ritter H W, Stemerick D M & Stewart K T, *J Med Chem*, 26 (1983) 431; (b) Ghatole A M, Lanjewar K R & Gaidhane M K, *J Pharm Res*, 5 (2012) 2758; (c) Ghatole A M, Lanjewar K R & Gaidhane M K, *Int J Res Biosciences*, *Agriculture & Technology*, 1 (2015) 89.
16 Dimmock J R & Kumar P, *Curr Med Chem*, 4, 1997, 1.
17 (a) Ghatole A M, Lanjewar K R, Gaidhane M K & Hatzade K M, *Spectrochim Acta Part A: Molecular and Biomolecular Spectroscopy*, 151 (2015) 515; (b) Ghatole A M, Lanjewar K R, Gaidhane M K & Hatzade K M, *Bulgarian J Science Education*, 29 (2020) 206.
18 Cordova A, *Accts Chem Res*, 37 (2004) 102.
19 Kleinmann E F, in *Comprehensive Organic Synthesis*. edited by Trost B M, Flemming T, Vol. 2. (Pergamon Press, New York) (1991).
20 Arend M, Westermann B & Risch N, *Angew Chem Int Ed*, 37 (1998) 1044.
21 Tramontini M & Angiolini L, *Tetrahedron*, 46 (1990) 1791.
22 Denmark S & Nicaise O J C, in *Comprehensive Asymmetric Catalysis*, edited by Pfaltz A, Jacobsen E N, Yamamoto H. (Verlag Berlin Heidelberg: Springer), 2 (1999) 93.
23 Kobayashi S & Ishitani H H, *Chem Rev*, 99 (1999) 1069.
24 Conticello S G, *Genome Biology*, 9(6) (2008) 229.
25 Refsland E W & Harris R S, *Curr Top Microbiol Immunol*, 371 (2013) 1.
26 Krejci A, Hupp T R, Lexa M, Vojtesek B & Muller P, *Bioinformatics*, 32(1) (2016) 9.
27 Seplyarskiy V B, Soldatov R A, Popadin K Y, Antonarakis S E & Bazykin G A, *Genome Res*, 26(2) (2016) 174.
28 Lipinski C A, Lombardo F, Dominy B W & Feeney P G, *Adv Drug Deliv Rev*, 46(1-3) (2001) 3.
29 Daina A & Zoete V A, *Chem Med Chem.*, 11(11) (2016) 1117.
30 Zahra S N E, Khattak N A & Mir A, *Theoretical Biology & Medical Modelling*, 10 (2013) 1.
31 Tabassum S, Zaki M, Afzal M & Arjmand A, *Eur J Med Chem*, 74 (2014) 509.
32 Shi K, Demir O, Carpenter M A, Wagner J & Kurahashi K, *Scientific Reports*, 7(1) (2017) 17415.
33 Yang B Li, Xiaosa L & Liqun C, *J Genet Genomics*, 44(9), 2017, 423.
34 Gordon C M, *Appl Catal A*: *General*, 222 (2001) 101.
35 Holbrey J D & Seddon K R, *Clean Product Processes*, 1 (1999) 223.
36 Wasserscheid P & Keim W, *Angew Chem*, 39(21) (2000) 3772.
37 Sheldon R A, *Chem Commun*, 2399 (2001).
38 Welton T, *Chem Rev*, 99 (1999) 2071.
39 Wenzel A & Jacobsen J E N, *J Am Chem Soc*, 124 (2002) 12964.
40 Katritzky A R, Qiu G, He H Y & Yang B J, *J Org Chem*, 65 (2000) 3683.
41 Manabe K, Mori Y, Wakabayashi T & Nagayama S, *J Am Chem Soc*, 122 (2000) 7202.
42 Manabe K, Mori Y & Kobayashi S, *Tetrahedron*, 57 (2001) 2537.
43 Cozzi P G, Simone B D & Umani-Ronchi A, *Tetrahedron Lett*, 37 (1996) 1691.
44 Kobayashi S. Araki M & Yasuda M, *Tetrahedron Lett*, 36 (1995) 5773.
45 Kobayashi S, Iwamoto S & Nagayama S, *Synlett*, 1099 (1997).
46 Kobayashi S, Busujima T & Nagayama S, *Synlett*, 545 (1999).
47 Akiyama T, Takaya J & Kagoshima H, *Synlett*, 1426 (1999).
48 Loh T P & Wei L L, *Tetrahedron Lett*, 39 (1998) 323.
49 Loh T P, Liung S B K W, Tan K L & Wei L L, *Tetrahedron*, 37 (2000) 3227.
50 Ojima I, *Catalytic Asymmetric Synthesis*, 2nd Edn. edited by I Ojima (Wiley-VCH, New York) (http:// www.wiley.com/). (2000), Pages: XIV, 864 Pages, Hardcover. Price: 169.- Euro / 330.54 DM / 294- SFR. ISBN: 0-471-29805-0, *Molecules: A Journal of Synthetic Chemistry and Natural Product Chemistry*, 6(12) (2001) 1013.
51 Daina A, Michielin O & Zoete V, *Sci Rep*, 7 (2017) 42717.
52 Ghose A K, Viswanadhan V N & Wendoloski J J, *J Comb Chem*, 1(1) (1999) 55.
53 Egan W J, Jr Merz K M & Baldwin J J, *J Med Chem*, 43(21) (2000) 3867.
54 Veber D F, Johson S R, Cheng H Y, Smith B R & Ward K W, *J Med Chem.*, 45(12) (2002) 2615.
55 Muegge I, Heald S L & Brittelli D, *J Med Chem.*, 44(12) (2001) 1841.
56 Brenk R, Schipani A, James D, Krasowski A & Gilbert I H, *Chem Med Chem.*, 3(3) (2008) 435.
57 Ogu C C & Maxa J L, *Proc* (*Bayl Univ Med Cent*), 13(4) (2000) 421.
58 Delaney J S, *J Chem Inf Comput Sci*, 44(3) (2004) 1000.
59 Fagerberg J H, Kaarlsson E, Ulander J, Hanisch G & Bergström C A, *Pharm Res*, 32(2) (2015) 578.
60 Chem Draw 3D Ultra Software.
61 Trott O & Olson A J, *J Comput Chem*, 31 (2010) 455.
62 Argus Lab 4.0.1 docking software.
63 Laskowski R A & Swindells M B, *J Chem Inf Model*, 51 (2011) 2778.